DESY 15-002, HU-EP-15/01, SFB/CPP-14-107

Leading-order hadronic contributions to the electron and tau anomalous magnetic moments

Florian Burger[a], Grit Hotzel[a], Karl Jansen[b], Marcus Petschlies[c]

[a] *Humboldt-Universität zu Berlin, Institut für Physik, Newtonstr. 15, D-12489 Berlin, Germany*
[b] *NIC, DESY, Platanenallee 6, D-15738 Zeuthen, Germany*
[c] *The Cyprus Institute, P.O.Box 27456, 1645 Nicosia, Cyprus*

Abstract

The leading hadronic contributions to the anomalous magnetic moments of the electron and the τ-lepton are determined by a four-flavour lattice QCD computation with twisted mass fermions. The continuum limit is taken and systematic uncertainties are quantified. Full agreement with results obtained by phenomenological analyses is found.

Keywords: quantum chromodynamics, lattice QCD, leptons, g-2, hadronic vacuum polarisation

1. Introduction

The standard model of particle physics (SM) contains three charged leptons l, mainly differing in mass, the electron, the muon, and the τ-lepton with $m_e : m_\mu : m_\tau \approx 1 : 207 : 3477$ [1]. Their magnetic moments, in particular their so-called anomalous magnetic moments, $a_l = (g-2)_l/2$, control their behaviour in an external magnetic field.
Being the lepton with the smallest mass the electron is stable. This leads to the electron magnetic moment being one of the most precisely determined quantities in nature. The agreement of the experimental and the SM value up to eight digits, see e.g. [2] and references therein, constitutes one of the cornerstone results for quantum field theories to be the correct mechanism for describing particle interactions. The very good agreement of the electron magnetic moment between experiment and SM calculations is not matched by the muon anomalous magnetic moment. In fact, here a two to four sigma discrepancy is observed, see e.g. [3]. One reason for the observed discrepancy could be that the magnetic moment of the muon receives larger non-perturbative contributions than the one of the electron. On the other hand, it is supposed to be also more sensitive to beyond the SM physics, since for a large class of theories new physics contributions are expected to be proportional to the squared lepton mass. Thus it is a prime candidate for detecting physics beyond the SM. Due to the large mass of the τ-lepton it would be the optimal lepton for finding new physics. However, because its lifetime is very short ($\mathcal{O}\left(10^{-13}\right)$s) there currently only exist bounds on its anomalous magnetic moment from indirect measurements [4].
The QED [5, 6] and the electroweak contributions [7, 8] to the lepton anomalous magnetic moments have been computed in perturbation theory to impressive five and two loops, respectively. The main uncertainties remaining in the theoretical determinations of the anomalous magnetic moments originate thus from the leading-order (LO) hadronic contributions. Since they are particularly sensitive to those virtual photon momenta that are of $\mathcal{O}\left(m_l^2\right)$, these contributions are inherently non-perturbative and not accessible to perturbation theory. In order to have a prediction of the anomalous magnetic moments from the SM alone, a non-perturbative method needs to be employed and the only such approach we presently know is lattice QCD (LQCD) which we use here.
As mentioned before, the hadronic LO contributions to the anomalous magnetic moments of the three SM leptons, a_l^{hvp}, strongly depend on the values of their masses. Since the magnitude of the lepton masses spans four orders of magnitude, the corresponding contributions to the anomalous magnetic moments differ substantially and probe very different energy regions, see also the discussion of Fig. 1 in Sect. 3.
In this article we present the results of our four-flavour computations of the quark-connected, LO hadronic vacuum polarisation contributions to the electron and τ-lepton anomalous magnetic moments obtained from the (maximally) twisted mass formulation of LQCD. The muon case has already been covered in [9]. One important feature of the present calculation is that we adopt exactly the same strategy as for the muon [9] including the same chiral and continuum extrapolations. Thus the results presented here are not only interesting in themselves but also serve as an important cross-check for our treatment of the hadronic vacuum polarisation function. Additionally to the sytematic uncertainties investigated in our previous paper, we quantify the light-quark disconnected contributions on one of our $N_f = 2+1+1$ ensembles. Another very important feature is that incorporating the complete first two generations of quarks enables us to directly and unambiguously compare our results with the values obtained from phenomenological analyses relying on experimental data and a dispersion relation. We note that the contributions from third-generation quarks can be neglected, since they are smaller than the current theoretical accuracy, as can be inferred e.g. from the data tables of Ref. [10]. Recently, the bottom quark contribution to a_μ^{hvp} has been explicitly computed on the lattice [11] confirming it to be one order of magnitude smaller than the current uncertainty of the phenomenological determinations of a_μ^{hvp}.
Additionally to the $N_f = 2 + 1 + 1$ flavour ensembles [12, 13] at unphysically large pion masses studied in [9], we computed the dominant light quark contributions to the anomalous magnetic moments on a $N_f = 2$ flavour ensemble directly at the physical point [14, 15]. This allows us to test the chiral extrapolations performed when using the reparametrisation introduced in [16, 17].

The next section comprises a short repetition of the most important equations needed to follow the discussion of the results for the LO hadronic vacuum polarisation contributions to the anomalous magnetic moments of the electron in Sect. 3 and the τ-lepton in Sect. 4. In Sect. 5 we summarise our results and draw our conclusions.

2. Computation of a_l^{hvp}

The LO hadronic contribution to the lepton anomalous magnetic moments, a_l^{hvp}, can be directly computed in Euclidean space-time according to [18, 19]

$$a_l^{\mathrm{hvp}} = \alpha^2 \int_0^\infty \frac{dQ^2}{Q^2} w\left(\frac{Q^2}{m_l^2}\right) \Pi_{\mathrm{R}}(Q^2) \,, \tag{1}$$

where α is the fine structure constant, Q^2 the Euclidean momentum, m_l the lepton mass, and $\Pi_{\mathrm{R}}(Q^2)$ the renormalised hadronic vacuum polarisation function,

$$\Pi_{\mathrm{R}}(Q^2) = \Pi(Q^2) - \Pi(0) \,.$$

It is obtained from the hadronic vacuum polarisation tensor

$$\Pi_{\mu\nu}(Q) = \int d^4x \, e^{iQ\cdot(x-y)} \langle J_\mu(x) J_\nu(y) \rangle = (Q_\mu Q_\nu - Q^2 \delta_{\mu\nu}) \Pi(Q^2) \,, \tag{2}$$

which is transverse because of the conservation of the electromagnetic current

$$J_\mu(x) = \frac{2}{3}\overline{u}(x)\gamma_\mu u(x) - \frac{1}{3}\overline{d}(x)\gamma_\mu d(x) + \frac{2}{3}\overline{c}(x)\gamma_\mu c(x) - \frac{1}{3}\overline{s}(x)\gamma_\mu s(x) \,. \tag{3}$$

Here u stands for the up quark, d for the down quark, c denotes the charm quark, and s the strange quark. Eq. (2) shows that $\Pi_{\mu\nu}(Q)$ results from the Fourier transformation of the correlator of two such currents. Taking up and down quarks together, since they are mass-degenerate in our setup, we decompose the quark-connected part of the hadronic vacuum polarisation tensor according to

$$\Pi_{\mu\nu}(Q) = \Pi^{\mathrm{ud}}_{\mu\nu}(Q) + \Pi^{\mathrm{s}}_{\mu\nu}(Q) + \Pi^{\mathrm{c}}_{\mu\nu}(Q) \,. \tag{4}$$

Hence, we can stepwise add the flavour contributions which will be done in the sections below. Since the definition in Eq. (1) results in a non-linear pion mass dependence for the light quarks, in [16, 17] a modified definition

$$a_l^{\mathrm{hvp}} = \alpha^2 \int_0^\infty \frac{dQ^2}{Q^2} w\left(\frac{Q^2}{H^2}\frac{H^2_{\mathrm{phys}}}{m_l^2}\right) \Pi_{\mathrm{R}}(Q^2) \tag{5}$$

has been proposed. H denotes some hadronic scale determined at unphysically high pion masses. For all flavours we choose as the hadronic scale the lowest lying ρ-meson state, m_V. $H = H_{\mathrm{phys}} = 1$ reproduces the standard definition in Eq. (1). Up to lattice artefacts the standard definition is also recovered at the physical value of the pion mass when the ratio H/H_{phys} becomes one. The weight function w is known from QED perturbation theory and is peaked at

$$Q^2_{\mathrm{peak}} = (\sqrt{5} - 2)\frac{H^2}{H^2_{\mathrm{phys}}} m_l^2 \,.$$

For a thorough description of the lattice calculation and a proof of automatic $\mathcal{O}(a)$ improvement of the vacuum polarisation function we refer to [9] and [20], respectively. In order to discuss systematic uncertainties later on, we briefly summarise our method of fitting the hadronic vacuum polarisation function here.

First, the lowest lying vector meson masses, m_i, and decay constants, f_i, are determined from the time dependence of the two-point function of the light, strange, and charm point-split vector current, individually, at zero spatial momentum. Then $\Pi(Q^2)$ determined in the momentum range between 0 and $Q^2_{\rm max}$ is split into a low-momentum part for $0 \leq Q^2 \leq Q^2_{\rm match}$ and a high-momentum one for $Q^2_{\rm match} < Q^2 \leq Q^2_{\rm max}$. The low-momentum fit function is given by

$$\Pi_{\rm low}(Q^2) = \sum_{i=1}^{M} \frac{f_i^2}{m_i^2 + Q^2} + \sum_{j=0}^{N-1} a_j (Q^2)^j \ , \tag{6}$$

and the high-momentum piece is parametrised as follows

$$\Pi_{\rm high}(Q^2) = \log(Q^2) \sum_{k=0}^{B-1} b_k (Q^2)^k + \sum_{l=0}^{C-1} c_l (Q^2)^l \ . \tag{7}$$

They are combined according to

$$\Pi(Q^2) = (1 - \Theta(Q^2 - Q^2_{\rm match}))\Pi_{\rm low}(Q^2) + \Theta(Q^2 - Q^2_{\rm match})\Pi_{\rm high}(Q^2) \ , \tag{8}$$

where $\Theta(x)$ is the Heaviside function.
This defines our so-called MNBC fit function. Our standard fit for the light and strange quark contributions is M1N2B4C1 which means $M = 1$, $N = 2$, $B = 4$, and $C = 1$ in Eqs. (6) and (7) above. As value of $Q^2_{\rm match}$ in the Heaviside functions in Eq. (8) we have chosen $2\,\mathrm{GeV}^2$. We have checked that varying the value of $Q^2_{\rm match}$ between $1\,\mathrm{GeV}^2$ and $3\,\mathrm{GeV}^2$ does not lead to observable differences as long as the transition between the low- and the high-momentum part of the fit is smooth. For the upper integration limit we use $Q^2_{\rm max} = 100\,\mathrm{GeV}^2$, since the integrals are saturated there as can be seen in Fig. 1 below.
Our analysis has been performed on the same set of gauge field configurations [12, 13] as have been used in our previous work [9]. A detailed list of the lattice parameters can be found there.

3. The electron $(g-2)$

The LO hadronic contribution to the electron anomalous magnetic moment $a_{\rm e}$ is dominated by momenta below $10^{-4}\,\mathrm{GeV}^2$. To a good approximation it can even be determined from the slope of the vacuum polarisation at zero momentum $a_{\rm e} \propto d\Pi/dQ^2(Q^2 = 0)$. Therefore, we only use the low-momentum part, $\Pi_{\rm low}(Q^2)$, of the hadronic vacuum polarisation function Eq. (6). The saturation of the integral for one of our ensembles, namely B55.32 featuring $m_{\rm PS} \approx 390\,\mathrm{MeV}$, $a \approx 0.08\,\mathrm{fm}$ and $L = 2.5\,\mathrm{fm}$, is shown in Fig. 1 for all three leptons by plotting

$$R_l(Q^2_{\rm max}) = \frac{a_l^{\rm hvp}(Q^2_{\rm max})}{a_l^{\rm hvp}(100\,\mathrm{GeV}^2)} \ , \tag{9}$$

where $a_l^{\rm hvp}(Q^2_{\rm max})$ is the LO hadronic contribution to the lepton anomalous magnetic moment integrated up to $Q^2_{\rm max}$. Fig. 1 also implies that for the electron we have to rely mostly on the extrapolation of our vacuum polarisation data to the small momentum region.

3.1. Contribution from up and down quarks

The light quark contribution is depicted in Fig. 2. Here, also the result at the physical value of the pion mass [14, 15] obtained with the standard definition Eq. (1) can be seen. This is fully compatible with the value determined by the linear extrapolation of the data obtained from the reparametrisation Eq. (5).

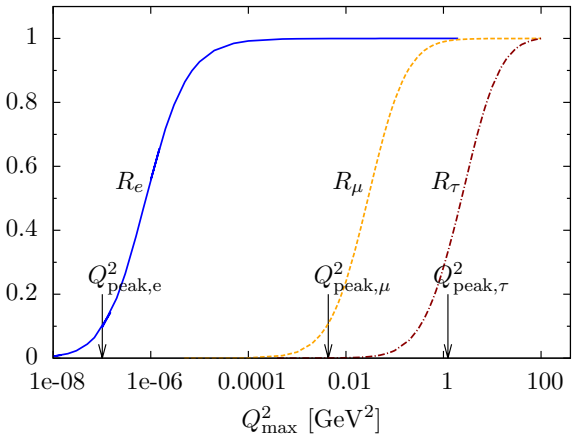

Figure 1: Comparison of the dependence on the upper integration bound in Eq. (5) of the four-flavour lepton anomalous magnetic moments. The blue curve represents the ratio defined in Eq. (9) for the electron, the orange one for the muon, and the dark red one for the tau. $Q^2_{\text{peak},l}$ denotes the momentum value where the kernel function in Eq. (5) attains its maximum.

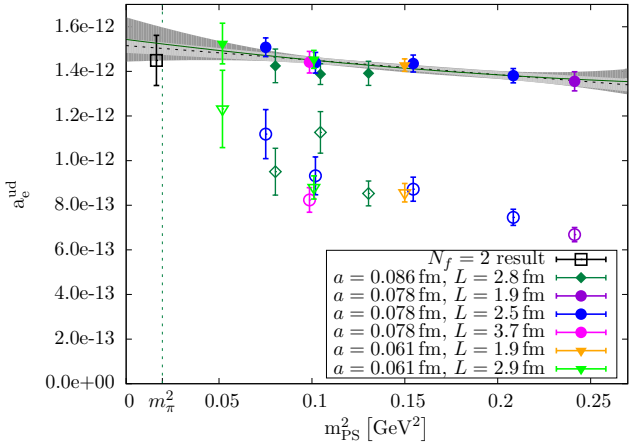

Figure 2: Light-quark contribution to a_e^{hvp} with filled symbols representing points obtained with Eq. (5), open symbols refer to those obtained with Eq. (1), i. e. $H = 1$. In particular, the two-flavour result at the physical point has been computed with the standard definition. The light grey errorband belongs to the linear fit, whereas the dark grey errorband is attached to the quadratic fit.

3.2. Adding the strange and the charm quark contributions

When incorporating the heavy, second-generation flavours, we have found that we have to take $\mathcal{O}(a^2)$ lattice artefacts into account. Hence, the four-flavour result for $a_{\mathrm{e}}^{\mathrm{hvp}}$ at the physical point in the continuum limit is obtained from simultaneously extrapolating in the pion mass, m_{PS}, and to zero lattice spacing a using

$$a^{\mathrm{hvp}}(m_{\mathrm{PS}}, a) = A + B\ m_{PS}^2 + C\ a^2 \tag{10}$$

with A, B, C denoting the free parameters of the fit. For $a_{\mathrm{e}}^{\mathrm{hvp}}$ the corresponding fit is shown in Fig. 3. Our result with only statistical uncertainty is

$$a_{\mathrm{e}}^{\mathrm{hvp}} = 1.78(06) \cdot 10^{-12}\ . \tag{11}$$

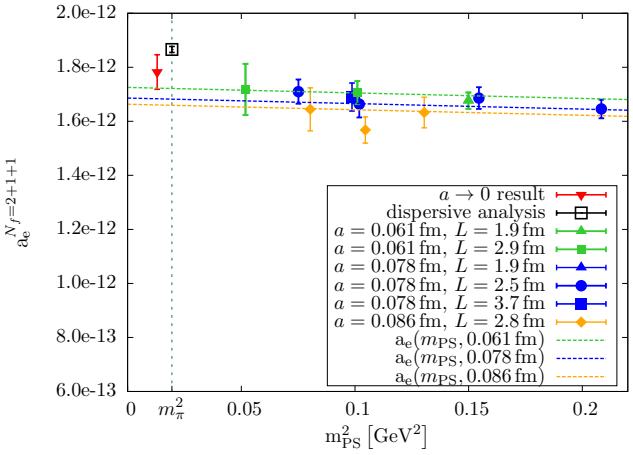

Figure 3: Chiral and continuum extrapolation of the $N_f = 2+1+1$ contribution to $a_{\mathrm{e}}^{\mathrm{hvp}}$. The inverted red triangle shows the value extrapolated to the continuum and to the physical value of the pion mass. It has been displaced to the left to facilitate the comparison with the dispersive result in the black square [21].

3.3. Systematic uncertainties

In this section we give an account of systematic uncertainties of our result for $a_{\mathrm{e}}^{\mathrm{hvp}}$ given in Eq. (11). We have investigated finite size effects (FSE), the dependence of our chiral extrapolation on the incorporation of large pion masses, vector meson fit ranges, and the dependence of our results on different vacuum polarisation fit functions. Moreover, for one ensemble the light quark-disconnected contribution is quantified.

3.3.1. Finite size effects

As described in detail in Ref. [9], the $N_f = 2 + 1 + 1$ ensembles analysed in this work feature $3.35 < m_{\mathrm{PS}}\ L < 5.93$, where L is the spatial extent of the lattice. Restricting our data to the condition $m_{\mathrm{PS}} L > 3.8$ yields

$$a_{\mathrm{e}}^{\mathrm{hvp}} = 1.77(07) \cdot 10^{-12} \tag{12}$$

after combined chiral and continuum extrapolation. This matches the result given in Eq. (11) and thus indicates that FSE are negligible in our computation. This finding is supported by comparing the results of two ensembles only differing in lattice size provided in Tab. 1. The numbers do not change when restricting the momenta of the larger ensemble to those of the smaller one. The FSE attributed to the lowest achievable momentum being $\frac{2\pi}{L}$ mixes with FSE entering the choice of different fit functions. We take a conservative approach and consider these effects separately.

Ensemble	$\left(\frac{L}{a}\right)^3 \times \frac{T}{a}$	$a_{\mathrm{e,ud}}^{\mathrm{hvp}}$	$a_{\mathrm{e}}^{\mathrm{hvp}}$
B35.32	$32^3 \times 64$	$1.44(05) \cdot 10^{-12}$	$1.66(05) \cdot 10^{-12}$
B35.48	$48^3 \times 96$	$1.44(05) \cdot 10^{-12}$	$1.69(05) \cdot 10^{-12}$

Table 1: Comparison of light-quark contribution to $a_{\mathrm{e}}^{\mathrm{hvp}}$ and total $a_{\mathrm{e}}^{\mathrm{hvp}}$ from ensembles of different volumes.

3.3.2. Chiral extrapolation

We have checked the validity of the chiral extrapolation by restricting the data, comprising pion masses between 227 MeV and 491 MeV, to the condition $m_{\mathrm{PS}} < 400\,\mathrm{MeV}$. The value we obtain

$$a_{\mathrm{e}}^{\mathrm{hvp}} = 1.78(07) \cdot 10^{-12} \tag{13}$$

only features a slightly larger uncertainty compared to the result in Eq. (11). Thus, we do not assign a systematic uncertainty to the usage of pion masses above 400 MeV.

3.3.3. Vector meson fit ranges

Our standard computation involves the determination of the masses and decay constants of the vector meson ground states for the different flavours. Their values depend on the choice of fit ranges. We have analysed different fit ranges for the two-point functions of the light, strange, and charm vector currents and propagated the uncertainties to the values for $a_{\mathrm{e}}^{\mathrm{hvp}}$. This showed that excited state contaminations are significant only for m_V and f_V determined from the light vector current-current correlator. Variations of the standard fit ranges by 0.1 fm to the left, right and both simultaneously do not lead to any observable differences in $a_{\mathrm{e}}^{\mathrm{hvp}}$ for the $\overline{s}\gamma_\mu s$- and the J/ψ correlator. Furthermore, the heavy flavour contributions are approximately one order of magnitude smaller than the light quark contribution such that their systematic uncertainties would not noticeably impact the overall uncertainty of $a_{\mathrm{e}}^{\mathrm{hvp}}$.

In the left panel of Fig. 4 the dependence of the light quark contribution to the electron anomalous magnetic moment on the fitrange for the ρ-correlator is plotted. Taking half the difference of the

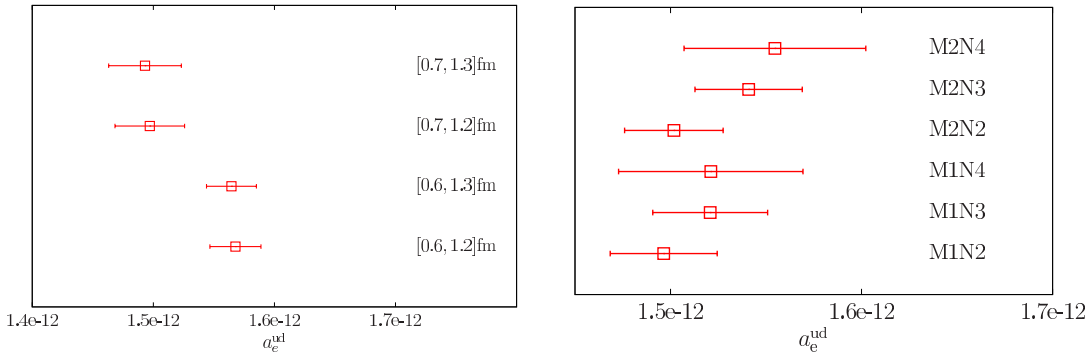

Figure 4: Dependence of $a_{\mathrm{e}}^{\mathrm{ud}}$ on the fitrange of the ρ-correlator (left panel) and on values chosen for M, N in the vacuum polarisation fit function (right panel). The standard ρ-correlator fit range is [0.7 fm, 1.2 fm] and the standard fit function corresponds to M1N2.

central values obtained for [0.6 fm, 1.2 fm] and [0.7 fm, 1.2 fm] gives a systematic uncertainty of

$$\Delta_V = 0.035 \cdot 10^{-12}\,. \tag{14}$$

3.3.4. Number of terms in MN fit function

The number of terms in the fit function Eq. (6) is given by M and N. M1N2 is our standard choice. Repeating the whole analysis with different numbers of terms leads to the results shown in the right panel of Fig. 4. We observe that all choices of M and N in Eq. (6) are compatible. Nevertheless,

we conservatively assign a systematic error by taking half the difference of the central values of the result of the M2N4 and the M1N2 fit. This leads to a systematic uncertainty of

$$\Delta_{MN} = 0.029 \cdot 10^{-12} \,. \tag{15}$$

For the heavy quarks the systematic uncertainties from different values of M and N turn out to be negligible.

3.3.5. Disconnected contributions

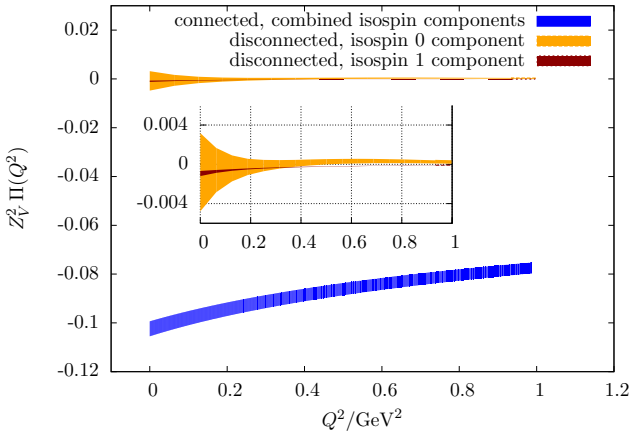

Figure 5: Comparison of the light quark contributions to the unsubtracted hadronic vacuum polarisation function from quark-connected and disconnected diagrams of the local current correlator. Z_V has been obtained from the ratio of the connected part of the conserved and local current-current correlators. The values have been computed with the analytical continuation method described in [22] without correcting for finite-size effects.

Leaving out the quark-disconnected contributions is a systematic uncertainty we cannot completely quantify, yet. We have started investigating their magnitude on the B55.32 ensemble mentioned already before. Using the local vector current we have detected a signal for the light quark part of the vacuum polarisation function when using 24 stochastic volume sources on 1548 configurations and 48 stochastic volume sources on 4996 configurations. Employing the one-end trick [23], the isovector part

$$\Pi^3_{\mu\nu}(x,y) = \langle J^3_\mu(x) J^3_\nu(y) \rangle \tag{16}$$

with $J^3_\mu = \frac{1}{2}\overline{\chi}\gamma_\mu\tau^3\chi$ is significantly different from zero. However, this is a pure lattice artefact and will not contribute in the continuum limit. On the other hand, the more interesting isoscalar part

$$\Pi^0_{\mu\nu}(x,y) = \frac{1}{9}\langle J^0_\mu(x) J^0_\nu(y) \rangle \tag{17}$$

with $J^3_\mu = \frac{1}{2}\overline{\chi}\gamma_\mu\mathbb{1}\chi$ is compatible with zero. The connected and disconnected pieces of the polarisation function for the light flavours are depicted in Fig. 5.
A comparison of the values of $a^{\mathrm{hvp}}_{l,\mathrm{ud}}$ for all three leptons on the B55.32 ensemble with and without incorporating the disconnected contributions is presented in Tab. 2. Here, we have combined the connected pieces obtained from the point-split current correlator with the isoscalar part of the disconnected contributions obtained from the local current correlator using the renormalisation constant Z_V determined from the ratio of the connected pieces of the conserved and the local vector current two-point functions. Therefore and because we only have results for one ensemble, the numbers below can only give hints on the influence of the disconnected pieces. We observe the tendency that for all three leptons $a^{\mathrm{hvp}}_{l,\mathrm{ud}}$ decreases when incorporating the disconnected contributions as has been predicted in [24]. However, this is statistically not significant. Furthermore, we find that the magnitude of the disconnected contributions is comparable to our current uncertainty. Hence, it will be mandatory to compute them when aiming at more precise results. For

the muon the value shifts by $\approx 3\%$, which is also not statistically significant at this stage, but is in accordance with the upper bound of $4-5\%$ given in [25].

	$a^{\rm hvp}_{\rm e,ud}$	$a^{\rm hvp}_{\mu,\rm ud}$	$a^{\rm hvp}_{\tau,\rm ud}$
without disc	$1.44(04)\cdot 10^{-12}$	$5.42(14)\cdot 10^{-8}$	$1.27(03)\cdot 10^{-6}$
with disc	$1.39(07)\cdot 10^{-12}$	$5.26(25)\cdot 10^{-8}$	$1.24(04)\cdot 10^{-6}$

Table 2: Comparison of light-quark contributions to $a_l^{\rm hvp}$ with and without disconnected pieces in the low-momentum region for the B55.32 ensemble. For all contributions the redefinition Eq. (5) and our standard analysis have been used.

The disconnected heavy flavour contributions need to be considered as well. We plan to check their size in future calculations. The pure charm quark contributions have been computed in perturbation theory and shown to be suppressed by a factor $\left(\frac{q^2}{4\ m_c^2}\right)^4$ [26], where q^2 is the relevant energy scale of the problem.

3.4. Comparison with the phenomenological value

Adding the quantified systematic uncertainties in quadrature we obtain as final result

$$a_{\rm e}^{\rm hvp} = 1.782(64)(45)\cdot 10^{-12}\ . \tag{18}$$

This can directly be compared with the phenomenological determination of [21]

$$a_{\rm e}^{\rm hvp} = 1.866(10)(05)\cdot 10^{-12}\ . \tag{19}$$

They are fully compatible with each other although our lattice result still is afflicted with larger errors.

4. The τ-lepton $(g-2)$

The large mass of the tau lepton, $m_\tau \approx 1.8\,\text{GeV}$, implies a peak of the weight function in the expression for the LO hadronic contribution to its magnetic moment in Eq. (1) at $Q^2_{\rm peak} = 0.745\,\text{GeV}^2$. This is very different from the peak position of the electron weight function. Hence $a_\tau^{\rm hvp}$ requires data from a different part of the vacuum polarisation function, in particular, also the high-momentum piece of our fit function Eq. (7) is important here.

4.1. Contribution from up an down quarks

As for the electron, we start off by showing the contribution of the first-generation flavours to $a_\tau^{\rm hvp}$ in Fig. 6. The data show a qualitatively similar behaviour to those of the electron in Fig. 2. Their values differ, however, by six orders of magnitude. In particular, we find that the data at unphysical pion masses obtained with Eq. (5), can be linearly extrapolated to the physical pion mass. This demonstrates again that the method of including $\frac{H}{H_{\rm phys}}$ in the weight function is advantageous for the chiral extrapolation. The value extrapolated in this way agrees with our calculation directly at the physical pion mass shown as the open square in Fig. 6.

4.2. Adding the strange and the charm quark contributions

As for the electron, we perform the chiral and continuum extrapolation of the complete four-flavour result using a fit of the form given in Eq. (10). It is shown in Fig. 7. Comparing this with Fig. 3, we see that the lattice artefacts are much smaller than for the electron such that we would have obtained a compatible result when omitting the a^2 term in Eq. (10). As can be seen in Figs. 8 and 9, for the tau lepton both, the strange and the charm contribution do not show significant cut-off effects and hence, also for the total contribution a^2 effects are small. We nevertheless perform the continuum extrapolation in order to use exactly the same analysis strategy as for the other leptons. Our four-flavour result with only statistical uncertainty reads

$$a_\tau^{\rm hvp} = 3.41(8)\cdot 10^{-6}\ . \tag{20}$$

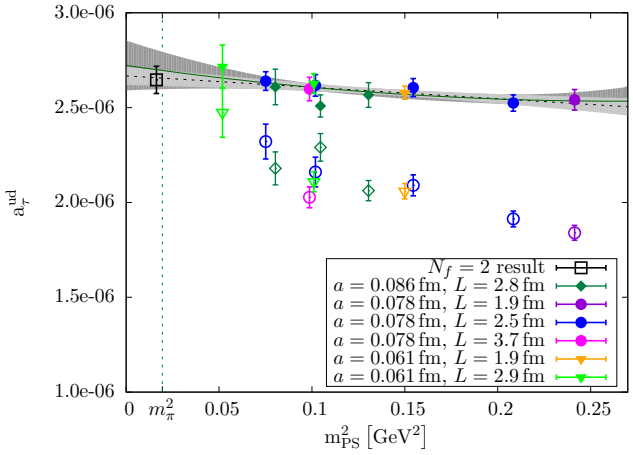

Figure 6: Light-quark contribution to $a_\tau^{\rm hvp}$ with filled symbols representing points obtained with Eq. (5), open symbols refer to those obtained with Eq. (1), i. e. $H = 1$. We note that the two-flavour result at the physical point has been computed with the standard definition. The light grey errorband belongs to the linear fit (dotted black line), whereas the dark grey errorband is attached to the quadratic fit (solid green line).

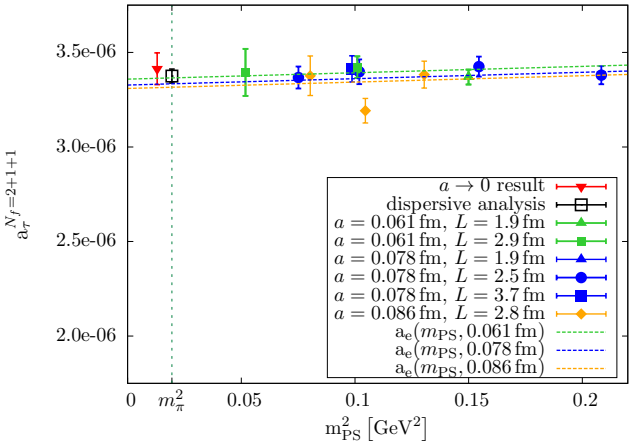

Figure 7: Chiral and continuum extrapolation of the $N_f = 2+1+1$ contribution to $a_\tau^{\rm hvp}$. The inverted red triangle shows the value in the continuum limit at the physical value of the pion mass. It has been displaced to the left to facilitate the comparison with the dispersive result depicted as black square [27].

4.3. Systematic uncertainties

We have investigated the same systematic uncertainties for our determination of $a_\tau^{\rm hvp}$ as for the case of the electron. The influence of the disconnected contributions has already been discussed in the section of $a_e^{\rm hvp}$.

4.3.1. Finite size effects

Restricting our data to the condition $m_{\rm PS}L > 3.8$ yields

$$a_\tau^{\rm hvp} = 3.40(09) \cdot 10^{-6}\,. \tag{21}$$

This is compatible with the result in Eq. (20). Comparing again the two ensembles at $m_{\rm PS} \approx 315\,\text{MeV}$ which only differ in the extent of the lattices also indicates negligible finite size effects as shown in Tab. 3. Hence, we do not assign a FSE related systematic uncertainty.

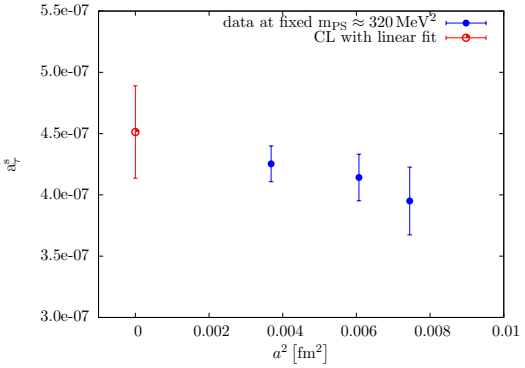

Figure 8: Continuum limit of strange quark contribution to a_τ^{hvp} at approximately fixed pion mass.

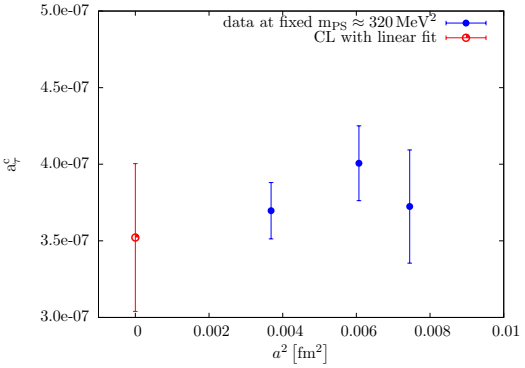

Figure 9: Continuum limit of charm quark contribution to a_τ^{hvp} at approximately fixed pion mass.

Ensemble	$\left(\frac{L}{a}\right)^3 \times \frac{T}{a}$	$a^{\mathrm{hvp}}_{\tau,\mathrm{ud}}$	a^{hvp}_{τ}
B35.32	$32^3 \times 64$	$2.62(06) \cdot 10^{-6}$	$3.40(07) \cdot 10^{-6}$
B35.48	$48^3 \times 96$	$2.60(06) \cdot 10^{-6}$	$3.41(07) \cdot 10^{-6}$

Table 3: Comparison of light-quark contribution to a_τ^{hvp} and total a_τ^{hvp} from ensembles of different volumes.

4.3.2. Chiral extrapolation

Restricting the analysed ensembles to those featuring pion masses $m_{\mathrm{PS}} < 400\,\mathrm{MeV}$, we get

$$a_\tau^{\mathrm{hvp}} = 3.45(09) \cdot 10^{-6}\ . \tag{22}$$

This is again compatible with the value given in Eq. (20). Hence, we do not assign a systematic uncertainty to the fact that ensembles with pion masses above 400 MeV have been employed when extrapolating to the phyical value of the pion mass.

4.3.3. Vector meson fit ranges

The situation is similar to the case of the electron reported above. Only the excited state contamination in the ρ-correlator has to be taken into account as systematic uncertainty. In the left panel of Fig. 10 the dependence of the light quark contribution, a_τ^{ud}, on the fit range chosen to extract the spectral information from the ρ-correlator is depicted.

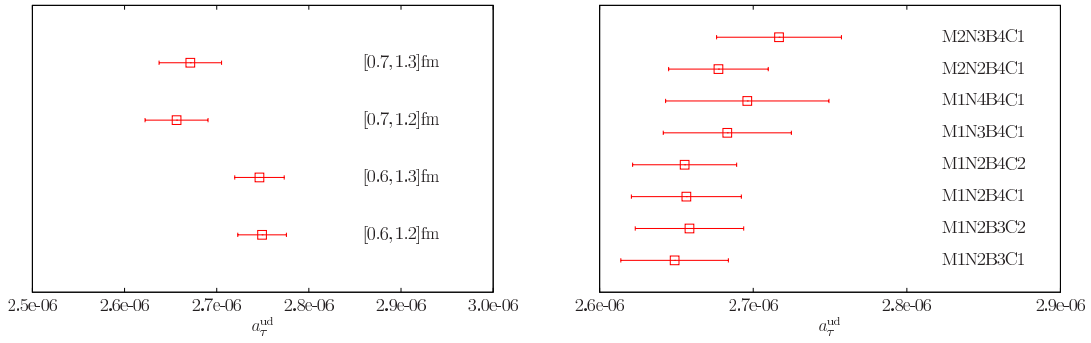

Figure 10: Dependence of a_τ^{ud} on the fit range of the ρ-correlator (left panel) and on the values chosen for M, N, B, and C in the vacuum polarisation fit function (right panel). The standard ρ-correlator fit range is $[0.7\,\mathrm{fm}, 1.2\,\mathrm{fm}]$ and the standard fit function corresponds to M1N2B4C1.

Taking half the difference of the central values obtained for $[0.6\,\mathrm{fm}, 1.2\,\mathrm{fm}]$ and our standard fit

range $[0.7\,\mathrm{fm}, 1.2\,\mathrm{fm}]$ results in an estimated systematic uncertainty of

$$\Delta_V = 0.046 \cdot 10^{-6} \,. \tag{23}$$

4.3.4. Number of terms in MNBC fit function
Due to the large Q^2_{peak} we have to take the whole vacuum polarisation function Eq. (8) into account, including in particular the high-momentum piece in Eq. (7). Thus, we have four different types of terms in the fit function that can have different numbers of summands. As for the electron, we only find observable differences in the light quark sector. But also here the results from different fits are all compatible as shown in the right panel of Fig. 10. Conservatively, we take half the difference between the M2N3B4C1 and M1N2B4C1 fit and assign a systematic uncertainty of

$$\Delta_{MNBC} = 0.030 \cdot 10^{-6} \tag{24}$$

to our choice of the fit function.

4.4. Comparison with the phenomenological value
Including the identified systematic uncertainties added in quadrature, our final four-flavour result reads

$$a_\tau^{\mathrm{hvp}} = 3.41(8)(5) \cdot 10^{-6} \,. \tag{25}$$

This agrees with the one obtained by a dispersive analysis [27]

$$a_\tau^{\mathrm{hvp}} = 3.38(4) \cdot 10^{-6} \,. \tag{26}$$

Compared to the electron even better agreement between the lattice and the phenomenological result is observed for the τ-lepton. In this case, the uncertainty of our twisted mass LQCD calculation is only about twice the phenomenological one.

5. Summary and Conclusions

In this article we have presented the first four-flavour LQCD computation of the LO hadronic vacuum polarisation contributions to the anomalous magnetic moments of the electron and the τ-lepton. Our results have been obtained with $N_f = 2 + 1 + 1$ twisted mass fermions mostly at unphysically large pion masses but, at least for the light quark contribution, also directly at the physical point. We find that for both, the electron and the tau lepton the chirally extrapolated values for the light quark contributions agree with the one at the physical point.
For our data at unphysically large values of the pion mass we have investigated the systematic uncertainties of the method used to obtain our final results. In particular, we have addressed the effects of non-zero lattice spacings, the finite volumes, the fit range for extracting the vector meson mass, and using different fit functions for the vacuum polarisation function. As an additional uncertainty we have investigated the disconnected contributions by using the local vector current. This led to the first observation of a signal for the disconnected diagrams which, however, is compatible with zero within our current errors and which we therefore have neglected. This will no longer be justified once the uncertainties of the connected pieces are reduced.
Our final results are summarised in the table below and agree with the phenomenological determinations of the electron and tau lepton magnetic moments which are also shown there. This constitutes another evidence that our analysis, also employed for the muon and described in more detail in [9], is correct.

	$a_{\mathrm{e}}^{\mathrm{hvp}}$	a_{μ}^{hvp}	a_{τ}^{hvp}
this work	$1.782(64)(45) \cdot 10^{-12}$	$6.78(24)(18) \cdot 10^{-8}$	$3.41(8)(5) \cdot 10^{-6}$
dispersive analyses	$1.866(10)(05) \cdot 10^{-12}$ [21]	$6.91(01)(05) \cdot 10^{-8}$ [28]	$3.38(4) \cdot 10^{-6}$ [27]

As in the case of the muon, also for the electron and tau lepton anomalous magnetic moment the errors of our calculations are still larger than those from the dispersive analyses quoted above. However, it can be expected that with future lattice QCD calculations at the physical value of the pion mass, increased statistics and an even better control over systematic uncertainties the phenomenological error can be matched, if not even beaten.

Acknowledgements

We thank the European Twisted Mass Collaboration (ETMC) for generating the gauge field ensembles used in this work. Special thanks goes to the authors of [29] who generously granted us access to their data for the disconnected contributions of the local vector current correlators. This work has been supported in part by the DFG Corroborative Research Center SFB/TR9. G.H. gratefully acknowledges the support of the German Academic National Foundation (Studienstiftung des deutschen Volkes e.V.) and of the DFG-funded Graduate School GK 1504. The numerical computations have been performed on the *SGI system HLRN-II* and the *Cray XC30 system HLRN-III* at the HLRN Supercomputing Service Berlin-Hannover, FZJ/GCS, BG/P, and BG/Q at FZ-Jülich.

References

[1] K. Olive, et al., Review of Particle Physics, Chin.Phys. C38 (2014) 090001. doi:10.1088/1674-1137/38/9/090001.

[2] G. Giudice, P. Paradisi, M. Passera, Testing new physics with the electron g-2, JHEP 1211 (2012) 113. arXiv:1208.6583, doi:10.1007/JHEP11(2012)113.

[3] N. Brambilla, S. Eidelman, P. Foka, S. Gardner, A. Kronfeld, et al., QCD and Strongly Coupled Gauge Theories: Challenges and Perspectives, Eur.Phys.J. C74 (10) (2014) 2981. arXiv:1404.3723, doi:10.1140/epjc/s10052-014-2981-5.

[4] J. Abdallah, et al., Study of tau-pair production in photon-photon collisions at LEP and limits on the anomalous electromagnetic moments of the tau lepton, Eur.Phys.J. C35 (2004) 159–170. arXiv:hep-ex/0406010, doi:10.1140/epjc/s2004-01852-y.

[5] T. Aoyama, M. Hayakawa, T. Kinoshita, M. Nio, Tenth-Order QED Contribution to the Electron g-2 and an Improved Value of the Fine Structure Constant, Phys.Rev.Lett. 109 (2012) 111807. arXiv:1205.5368, doi:10.1103/PhysRevLett.109.111807.

[6] T. Aoyama, M. Hayakawa, T. Kinoshita, M. Nio, Complete Tenth-Order QED Contribution to the Muon g-2, Phys.Rev.Lett. 109 (2012) 111808. arXiv:1205.5370, doi:10.1103/PhysRevLett.109.111808.

[7] A. Czarnecki, B. Krause, W. J. Marciano, Electroweak Fermion loop contributions to the muon anomalous magnetic moment, Phys.Rev. D52 (1995) 2619–2623. arXiv:hep-ph/9506256, doi:10.1103/PhysRevD.52.R2619.

[8] A. Czarnecki, B. Krause, W. J. Marciano, Electroweak corrections to the muon anomalous magnetic moment, Phys.Rev.Lett. 76 (1996) 3267–3270. arXiv:hep-ph/9512369, doi:10.1103/PhysRevLett.76.3267.

[9] F. Burger, X. Feng, G. Hotzel, K. Jansen, M. Petschlies, et al., Four-Flavour Leading-Order Hadronic Contribution To The Muon Anomalous Magnetic Moment, JHEP 1402 (2014) 099. arXiv:1308.4327, doi:10.1007/JHEP02(2014)099.

[10] M. Benayoun, P. David, L. DelBuono, F. Jegerlehner, An Update of the HLS Estimate of the Muon g-2, Eur.Phys.J. C73 (2013) 2453. arXiv:1210.7184, doi:10.1140/epjc/s10052-013-2453-3.

[11] B. Colquhoun, R. Dowdall, C. Davies, K. Hornbostel, G. Lepage, The Υ and Υ' Leptonic Widths, a_μ^b and m_b from full lattice QCDarXiv:1408.5768.

[12] R. Baron, et al., Light hadrons from lattice QCD with light (u,d), strange and charm dynamical quarks, JHEP 06 (2010) 111. arXiv:1004.5284, doi:10.1007/JHEP06(2010)111.

[13] R. Baron, et al., Computing K and D meson masses with $N_f = 2+1+1$ twisted mass lattice QCD, Comput.Phys.Commun. 182 (2011) 299–316. arXiv:1005.2042, doi:10.1016/j.cpc.2010.10.004.

[14] A. Abdel-Rehim, P. Boucaud, N. Carrasco, A. Deuzeman, P. Dimopoulos, et al., A first look at maximally twisted mass lattice QCD calculations at the physical point, PoS LATTICE2013 (2013) 264. arXiv:1311.4522.

[15] A. Abdel-Rehim, C. Alexandrou, P. Dimopoulos, R. Frezzotti, K. Jansen, et al., Progress in Simulations with Twisted Mass Fermions at the Physical Point, PoS LATTICE2014 (2014) 119. arXiv:1411.6842.

[16] X. Feng, K. Jansen, M. Petschlies, D. B. Renner, Two-flavor QCD correction to lepton magnetic moments at leading-order in the electromagnetic coupling, Phys.Rev.Lett. 107 (2011) 081802. arXiv:1103.4818, doi:10.1103/PhysRevLett.107.081802.

[17] D. B. Renner, X. Feng, K. Jansen, M. Petschlies, Nonperturbative QCD corrections to electroweak observablesarXiv:1206.3113.

[18] B. Lautrup, A. Peterman, E. de Rafael, Recent developments in the comparison between theory and experiments in quantum electrodynamics, Phys.Rept. 3 (1972) 193–260. doi:10.1016/0370-1573(72)90011-7.

[19] T. Blum, Lattice calculation of the lowest order hadronic contribution to the muon anomalous magnetic moment, Phys.Rev.Lett. 91 (2003) 052001. arXiv:hep-lat/0212018, doi:10.1103/PhysRevLett.91.052001.

[20] F. Burger, G. Hotzel, K. Jansen, M. Petschlies, The hadronic vacuum polarization and automatic O(a) improvement for twisted mass fermionsarXiv:1412.0546.

[21] D. Nomura, T. Teubner, Hadronic contributions to the anomalous magnetic moment of the electron and the hyperfine splitting of muonium, Nucl.Phys. B867 (2013) 236–243. arXiv:1208.4194, doi:10.1016/j.nuclphysb.2012.10.001.

[22] X. Feng, S. Hashimoto, G. Hotzel, K. Jansen, M. Petschlies, et al., Computing the hadronic vacuum polarization function by analytic continuation, Phys.Rev. D88 (2013) 034505. arXiv:1305.5878, doi:10.1103/PhysRevD.88.034505.

[23] P. Boucaud, et al., Dynamical Twisted Mass Fermions with Light Quarks: Simulation and Analysis Details, Comput. Phys. Commun. 179 (2008) 695–715. arXiv:0803.0224, doi:10.1016/j.cpc.2008.06.013.

[24] M. Della Morte, A. Juttner, Quark disconnected diagrams in chiral perturbation theory, JHEP 1011 (2010) 154. arXiv:1009.3783, doi:10.1007/JHEP11(2010)154.

[25] A. Francis, V. Gulpers, B. Jager, H. Meyer, G. von Hippel, et al., The leading disconnected contribution to the anomalous magnetic moment of the muon, PoS LATTICE2014 (2014) 128. arXiv:1411.7592.

[26] S. Groote, A. Pivovarov, Low-energy gluon contributions to the vacuum polarization of heavy quarks, JETP Lett. 75 (2002) 221. arXiv:hep-ph/0103047, doi:10.1134/1.1478517.

[27] S. Eidelman, M. Passera, Theory of the tau lepton anomalous magnetic moment, Mod.Phys.Lett. A22 (2007) 159–179. arXiv:hep-ph/0701260, doi:10.1142/S0217732307022694.

[28] F. Jegerlehner, R. Szafron, $\rho^0 - \gamma$ mixing in the neutral channel pion form factor F_π^e and its role in comparing e^+e^- with τ spectral functions, Eur.Phys.J. C71 (2011) 1632. arXiv:1101.2872, doi:10.1140/epjc/s10052-011-1632-3.

[29] C. Michael, K. Ottnad, C. Urbach, η and η' mixing from Lattice QCD, Phys.Rev.Lett. 111 (18) (2013) 181602. arXiv:1310.1207, doi:10.1103/PhysRevLett.111.181602.